Yield strength of α-silicon nitride at high pressure and high temperature

J. Qian,[1] C. Pantea,[1] J. Zhang,[1] L. L. Daemen,[1] Y. Zhao,[1] M. Tang,[1] T. Uchida,[2] Y. Wang[2]

[1] Los Alamos National Laboratory, Los Alamos, NM 87545, U.S.A; [2] Center for Advanced Radiation Sources, The University of Chicago, IL 60637, U.S.A

Introduction

Due to its covalent bonding, silicon nitride (Si_3N_4) exhibits high hardness, high wear resistance, low electrical conductivity, extraordinary chemical inertness, and high thermal stability.[1-3] Today, Si_3N_4 is one of the key engineering ceramics widely used in machining and in the semiconductor and aerospace industries. In addition to the development of fabrication techniques such as hot pressing,[4-5] gas pressure sintering,[6] high pressure-high temperature sintering,[7] and chemical vapor deposition methods,[8] sustained efforts have been devoted to discovering new phases of Si_3N_4 experimentally[9-12] and to elucidating the fundamental electronic structure and bonding theoretically.[13-14] Four polymorphs of Si_3N_4 have been reported so far, including two hexagonal phases (α and β-Si_3N_4), a cubic spinel structure (c-Si_3N_4), and another still ambiguous phase (δ-Si_3N_4).[10] Extensive work has been performed in studying the mechanical properties,[15-18] phase transition,[19-21] and equation of state[22] of Si_3N_4. However, one of the fundamental parameters of Si_3N_4 — the yield strength at high pressure-high temperature conditions is still lacking. This information is critical for evaluating the performance of Si_3N_4 in a real working (load and high temperature) environment. In this work, we investigate the yield strength of α-Si_3N_4 at pressures up to 9.2 GPa and temperatures up to 1234°C through the analysis of the shape of x-ray diffraction lines from a powdered sample.

Methods and Materials

α-Si_3N_4 powder (purity >90%, grain size 50~100 nm) was purchased from Alfa Aesar. Two separated layers of α-Si_3N_4 and NaCl powder were loaded inside a hexagonal BN capsule, which was placed in an amorphous carbon furnace. NaCl worked as the internal pressure standard and pressure was calculated from Decker's equation of state for NaCl.[23] The temperature was measured by a $W_{25}Re_{75}$ — W_3Re_{97} thermocouple which was positioned at the center of the furnace and was in direct contact with the α-Si_3N_4 sample and NaCl layers; no correction was made for the pressure effect on the thermocouple emf. In situ energy-dispersive synchrotron x-ray diffraction experiments were performed at the bending magnet beamline (13-BM-D) at the GSECARS facility of the Advanced Photon Source using the 250-ton multi-anvil press with the DIA-type cubic anvil apparatus.[24] The incident x-ray beam was collimated to a rectangular cross-section with dimensions 100×200 μm, and the diffracted x-ray signal was collected by a Ge solid state detector at a fixed angle of $2\theta = 5.857°$. The sample was compressed to 9.2 GPa at room temperature and then heated to 1234°C under constant load. The x-ray diffraction patterns were collected at α-Si_3N_4 and NaCl locations very close to the thermocouple junction at different pressure-temperature conditions. The obtained energy-dispersive diffraction data were analyzed with the Plot85 software package.

The stress and strength of α-Si_3N_4 can be derived from the peak broadening in the x-ray diffraction patterns. The detailed method is outlined by Weidner et al. based on two facts: microscopic deviatoric stress is the origin of x-ray line broadening in addition to grain size, and yielding occurs through the redistribution of the deviatoric stress over the entire sample at a certain high stress level.[25] In the case of diffraction lines with Gaussian profiles, the combination of grain size and strain broadening can be described by[26]

$$[\beta(E)]^2 = \left[\frac{Khc}{2L\sin\theta}\right]^2 + (\varepsilon E)^2,$$

where $\beta(E)$ is the peak broadening at the photon energy E, K the Scherrer constant, h Planck's constant, c the velocity of light, L the average grain size, and ε the differential strain. Therefore, differential strain and average grain size can be derived from the slope and ordinate intercept of the plot of $[\beta(E)]^2$ against E^2, respectively.

Results

The (110) and (101) diffraction peaks of α-Si_3N_4 are displayed in Fig. 1 at four different points along the experimental pressure-temperature path. During the compression from ambient up to 9.2 GPa at room temperature, the α-Si_3N_4 peaks broaden asymmetrically, with a much more severe broadening on the small d-spacing side of the peak — see the bottom three curves in Fig. 1.

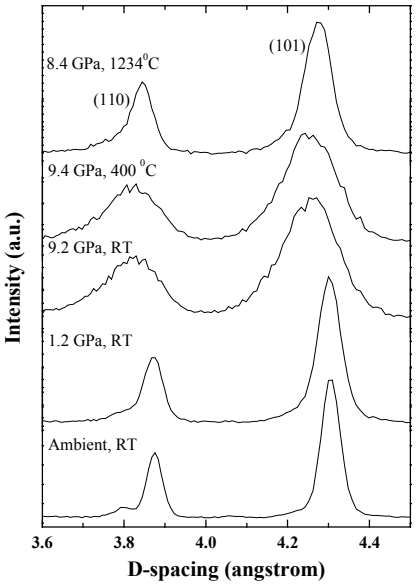

Fig. 1 (110) and (101) diffraction lines of α-Si_3N_4 at selected pressure and temperature conditions.

This indicates that the applied pressure is supported only by the bridged parts of the α-Si_3N_4 grains. Meanwhile, at this stage,

the generated stress is not large enough to cause any yielding. Similar behavior was observed for diamond and moissanite during compression up to 10 and 11.8 GPa, respectively.[25, 27] During heating at constant load, both (110) and (101) peaks of α-Si_3N_4 remain almost unchanged up to 400°C. The peaks narrow and become more symmetric at temperatures above 400°C, which is a clear evidence of yielding accompanied by stress redistribution over the entire sample — see the top two curves in Fig. 1.

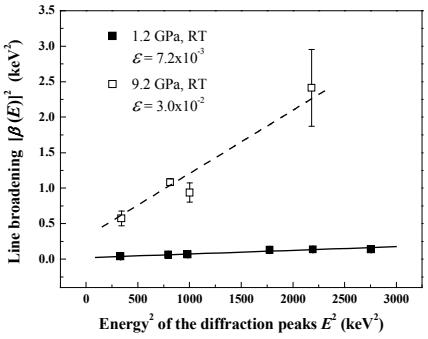

Fig. 2 Energy-dependent line broadening of α-Si_3N_4 at two different pressures at room temperature.

Figure 2 shows the plot of $[\beta(E)]^2$ as a function of E^2 for two selected pressure-temperature conditions. Due to the co-existence of the NaCl pressure standard, h-BN capsule, and α-Si_3N_4 in the sample chamber, diffraction peaks from these different phases tend to overlap, and this complicates the extraction of peak width, especially with broadened peaks at high-pressure conditions. For a better statistics, five α-Si_3N_4 diffraction lines are selected for peak broadening analysis, and the error bar represents the standard deviation. There are relatively large uncertainties about the line broadening of some of the α-Si_3N_4 peaks, but it is still obvious that a linear fit is suitable for the plot of $[\beta(E)]^2$ against E^2 even for the worst case scenario, shown as the top blank square plot fitted with a dash line in Fig. 2. Better precision of line broadening and more accurate deduction of grains size and differential strain can be obtained with angle dispersive diffraction and monochromatic synchrotron beam, which requires a much complicate instrumentation for the multi-anvil press.

The grain size, especially when it goes down to nanometer range, contributes significantly to the diffraction line broadening.[28] Given the intrinsic brittleness of the α-Si_3N_4,[2, 5, 17] we believe it was worthwhile to explore possible grain size reduction during compression. Additionally, we thought that more details about the dependence of the differential strain as a function of pressure and/or temperature could be revealed by introducing the grain size in the same plot.

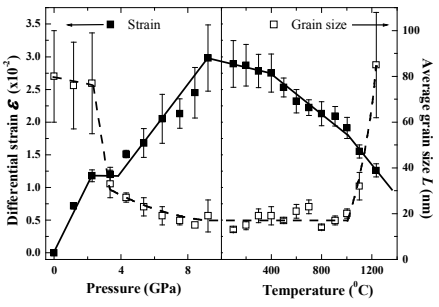

Fig. 3 Differential strain (full square) and average grain size (blank square) of α-Si_3N_4 at various pressure and temperature conditions.

Figure 3 shows the differential strain and average grain size at various pressure and temperature conditions as full and blank square plots with solid and dash guide lines, respectively. The nearly linear dependence of the strain on pressure up to 9.2 GPa at room temperature indicates that the compression process is elastic. The plateau around the pressure of 3 GPa is clearly associated with a dramatic grain size reduction approximately from 80 to 30 nm. It is intuitive to envision that grain fracture rearranges local grain-to-grain contact and eases the strain growth temporarily at this particular region during loading. Afterward, there is an average grain size reduction from 30 to 20 nm upon further compressing from 3.4 to 9.2 GPa, but it seems that this small grain size reduction has no effect on the dependence of differential strain on pressure.

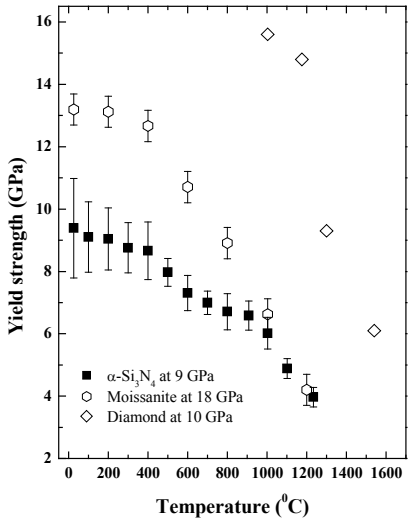

Fig. 4 Yield strength of α-Si_3N_4 (square) as a function of temperature at a pressure of 9 GPa. The strength data for moissanite (hexagon) and diamond (diamond) are also plotted for comparison.

Discussion

As temperature is increased to 400°C at constant load, there is a slight negative slope in the differential strain, which is probably caused by thermally induced strain relaxation since there is a small increase of the internal cell pressure in this region. Above 400°C, α-Si_3N_4 starts yielding and the strain drops rapidly with further heating to 1234°C. It is essential to point out here that $\alpha \rightarrow \beta$-Si_3N_4 transformation is an important issue at high pressure-high temperature conditions,[19-21] and there is no apparent $\alpha \rightarrow \beta$-Si_3N_4 transformation in our experiment up to 8.4 GPa and 1234°C. The grain size of α-Si_3N_4 remains around 20 nm upon heating all the way to 1000°C, above which there is a fast grain growth. The final grain size at 1234°C is about 80 nm, which is very close to the initial grain size. Rapid grain growth (by about one order of magnitude) has been reported around 1000°C during the crystallization of amorphous Si_3N_4.[7] Simultaneously, at 1000°C, the strain starts decreasing more rapidly. This coincidence can be explained by α-Si_3N_4 grain growth (which should be facilitated by the presence of small grains at that stage of the experiment). Indeed, grain growth reduces grain-to-grain contact sites and accelerates the differential strain diminution.

For α-Si_3N_4, the preceding results clearly demonstrate that the grain size information is critical in understanding the detailed evolution of differential strain at high pressure-high temperature. It is necessary to mention that the average grain size here is the x-ray scattering domain size (crystallite size), which may not represent the crystal size of α-Si_3N_4. Further experimental investigations in other ceramics are needed to confirm the importance of simultaneously determining stress and grain size in differential strain studies.

Given that the differential stress which can be sustained by the grains represents the yield strength after the yielding of α-Si_3N_4 at 400°C, the yield strength of α-Si_3N_4 can be determined from multiplying the differential strain by its aggregate Young's modulus, 315 GPa, which is calculated from the bulk modulus of 229 GPa based on the equation of state study by Kruger et. al[22] and a Poisson's ratio of 0.27.

The yield strength of α-Si_3N_4 as a function of temperature at 9 GPa is shown in Fig. 4. Data for moissanite and diamond are also plotted for comparison. The yield strength of α-Si_3N_4 decreases from 8.7 GPa at 400°C to 4.0 GPa at 1234°C. Compared to the yield strength of moissanite (12.8 at 400°C),[27] α-Si_3N_4 is much weaker at relatively low temperatures (below 800°C). The comparison with diamond (with yield strength above 16 GPa at the onset temperature of 1000°C) is even less favorable.[25

We demonstrated the dependence of strain on pressure and temperature through the analysis of peak broadening of the energy-dispersive diffraction data for α-Si_3N_4. The "fine structure" of the evolution of strain can be explicated with the complementary information delivered by the grain size variation. The yield strength of α-Si_3N_4 is low initially (less than 9 GPa at 400°C). Although it becomes comparable to moissanite at temperatures above 1000°C, the low onset temperature of yielding (400°C) and the deterioration of strength upon further increase of temperature will set a limitation on the performance of α-Si_3N_4 as an engineering material. Nevertheless, a better understanding about the correlation between yield strength and grain size could be extremely helpful to design functional ceramics through a deliberate configuration of grains with various size in the near future.

Acknowledgement

This work was completed under the auspices of the U.S. Department of Energy (DoE) under contract W-7405-ENG-36 with the University of California. The Los Alamos National Laboratory research projects are supported by the DoE-OIT_IMF and DoD/DoE_MOU programs. The experimental part of this work was performed at GeoSoilEnviroCARS (Sector 13), Advanced Photon Source (APS), Argonne National Laboratory, which is supported by the National Science Foundation — Earth Sciences (EAR-0217473), Department of Energy — Geosciences (DE-FG02-94ER14466), and the State of Illinois. Use of the APS is supported by the U.S. Department of Energy, Basic Energy Sciences, and Office of Energy Research, under Contract No. W-31-109-Eng-38.

References

[1] A. Kelly, N. H. Macmillan, Strong Solids, Oxford University Press, New York (1986).

[2] J. B. Wachtman, Mechanical Properties of Ceramics, Chapter 24, John Wiley & Sons, New York (1996).

[3] A. J. Pyzik, D. F. Carroll, Annu. Rev. Mater. Sci., **24**, 189-214 (1994).

[4] G. Himsolt, H. Knoch, H. Huebner, and F. Kleinlein, J. Am. Ceram. Soc., **62** [1-2] 29-32 (1979).

[5] I. Tanaka, G. Pezzotti, T. Okamoto, and Y. Miyamoto, J. Am. Ceram. Soc., **72**, 1656-1660 (1989).

[6] M. Mitomo and S. Uenosono, J. Mater. Sci., **26**, 3940-44 (1991).

[7] Y. Li, Y. Liang, F. Zheng, X. Ma, and S. Cui, J. Mater. Res., **15** [4] 988-994 (2000).

[8] J. Yota, J. Hander, and A. A. Saleh, J. Vac. Sci. Technol. A, **18** [2] 372-276 (2000).

[9] A. Zerr, G. Miehe, G. Serhgiou, M. Schwarz, E. Kroke, R. Riedel, H. Fueb, P. Kroll, and R. Boehler, Nature, **400**, 340-342 (1999).

[10] A. Zerr, Phys. Stat. Sol. (b), **227** [2] R4-R6 (2001).

[11] T. Sekine, H. He, T. Kobayashi, M. Zhang and F. Xu, Appl. Phys. Lett., **76** [25] 3706-3708 (2000).

[12] M. Schwarz, G. Miehe, A. Zerr, E. Krobe, B. T. Poe, H. Fuess, and R. Riedel, Adv. Mater., **12** [12] 883-887 (2000).

[13] S. Mo, L. Ouyang, W. Y. Ching, I. Tanaka, Y. Koyama, and R. Riedel, Phys. Rev. Lett., **83** [24] 5046-5049 (1999).

[14] W. Y. Ching, L. Ouyang, and J. D. Gale, Phys. Rev. B., **61** [13] 8696-8700 (2000).

[15] I. Tanaka, F. Oba, T. Sekine, E. Ito, A. Kubo, K. Tatsumi, H. Adachi, and T. Yamamoto, J. Mater. Res., **17** [4] 731-733 (2002).

[16] J. Z. Jiang, H. Lindelov, L. Gerward, K. Stahl, J. M. Recio, P. Mori-Sanchez, S. Carlson, M. Mezouar, E. Dooryhee, A. Fitch, and D. J. Frost, Phys. Rev. B., **65**, 161202(R) (2002).

[17] K. Ogawa, F. Sugiyama, G. Pezzotti, and T. Nishida, J. Am. Ceram. Soc., **81** [1] 166-172 (1998).

[18] N. Hirosaki, Y. Akimune, and M. Mitomo, J. Am. Ceram. Soc., **77** [4] 1093-97 (1994).

[19] N. V. Danilenko, G. S. Oleinik, V. D. Dobrovol'skii, V. F. Britun, and N. P. Semenenko, Soviet Powder Metallurgy and Metal Ceramics, **31** [12] 1035-1040 (1992).

[20] H. He, T. Sekine, T. Kobayashi, and H. Hirosaki, Phys. Rev. B., **62** [17] 11412-11417 (2000).

[21] H. Suematsu, M. Mitomo, T. E. Mitchell, J. Petrovic, O. Fukunaga, and N. Ohashi, J. Am. Ceram. Soc., **80** [3] 615-20 (1997).

[22] M. B. Kruger, J. H. Nguyen, Y. M. Li, W. A. Caldwell, M. H. Manghnani, and R. Jeanloz, Phys. Rev. B., **55** [6] 3456-3460 (1997).

[23] D. L. Decker, J. Appl. Phys., **42**, 3239-3244 (1971).

[24] D. J. Weidner, M. T. Vaughan, J. Ko, Y. Wang, X. Liu, A. Yeganeh-haeri, R. E. Pacalo, and Y. Zhao, High-Pressure Research: Application to Earth and Planetary Sciences, Vol. **67**, pp. 13-17. Edited by Y. Syono and M. H. Manghnani, Geophysics Monograph Series, AGU, Washington DC (1992).

[25] D. J. Weidner, Y. Wang, and M. T. Vaughan, Science, **266**, 419-422 (1994).

[26] L. Gerward, S. Morup, and H. Topsoe, J. Appl. Phys., **47** [3] 822-825 (1976).

[27] J. Zhang, L. Wang, D. J. Weidner, T. Uchida, and J. Xu, American Mineralogist, **87**, 1005-1008 (2002).

[28] H. P. Klug and L. E. Alexander, X-ray Diffraction Procedures For Polycrystalline and Amorphous Materials, John Wiley & Sons, New York (1974).